

Antitumoral effects of 9-*cis* retinoic acid in adrenocortical cancer

Diana Rita Szabó · Kornélia Baghy · Peter M. Szabó · Adrienn Zsippai · István Marczell · Zoltán Nagy · Vivien Varga · Katalin Éder · Sára Tóth · Edit I. Buzás · András Falus · Ilona Kovalszky · Attila Patócs · Károly Rác · Peter Igaz

Received: 25 March 2013 / Revised: 10 June 2013 / Accepted: 11 June 2013 / Published online: 27 June 2013
© Springer Basel 2013

Abstract The currently available medical treatment options of adrenocortical cancer (ACC) are limited. In our previous meta-analysis of adrenocortical tumor genomics data, ACC was associated with reduced retinoic acid production and retinoid X receptor-mediated signaling. Our objective has been to study the potential antitumoral effects of 9-*cis* retinoic acid (9-*cis*RA) on the ACC cell line NCI-H295R and in a xenograft model. Cell proliferation, hormone secretion, and gene expression have been studied in the NCI-H295R cell line. A complex bioinformatics approach involving pathway and network analysis has been performed. Selected genes have been validated by real-time qRT-PCR. Athymic nude mice xenografted with NCI-H295R have been used in a pilot

in vivo xenograft model. 9-*cis*RA significantly decreased cell viability and steroid hormone secretion in a concentration- and time-dependent manner in the NCI-H295R cell line. Four major molecular pathways have been identified by the analysis of gene expression data. Ten genes have been successfully validated involved in: (1) steroid hormone secretion (*HSD3B1*, *HSD3B2*), (2) retinoic acid signaling (*ABCA1*, *ABCG1*, *HMGCR*), (3) cell-cycle damage (*GADD45A*, *CCNE2*, *UHRF1*), and the (4) immune response (*MAP2K6*, *ILIR2*). 9-*cis*RA appears to directly regulate the cell cycle by network analysis. 9-*cis*RA also reduced tumor growth in the in vivo xenograft model. In conclusion, 9-*cis*RA might represent a promising new candidate in the treatment of hormone-secreting adrenal tumors and adrenocortical cancer.

Electronic supplementary material The online version of this article (doi:10.1007/s00018-013-1408-z) contains supplementary material, which is available to authorized users.

D. R. Szabó · A. Zsippai · I. Marczell · Z. Nagy · V. Varga · K. Rác · P. Igaz (✉)
2nd Department of Medicine, Faculty of Medicine, Semmelweis University, Szentkirályi Str. 46, Budapest 1088, Hungary
e-mail: igaz.peter@med.semmelweis-univ.hu

K. Baghy · I. Kovalszky
1st Department of Pathology and Experimental Cancer Research, Faculty of Medicine, Semmelweis University, Üllői Str. 26, Budapest 1088, Hungary

P. M. Szabó · A. Patócs
Molecular Medicine Research Group, Hungarian Academy of Sciences and Semmelweis University, Szentkirályi Str. 46, Budapest 1088, Hungary

K. Éder · S. Tóth · E. I. Buzás · A. Falus
Department of Genetics, Cell- and Immunobiology, Faculty of Medicine, Semmelweis University, Nagyvárad Sq. 4, Budapest 1089, Hungary

Keywords Adrenocortical cancer · 9-*cis* retinoic acid · Hormone production · Microarray · Xenograft · Tumor growth

Introduction

Adrenocortical carcinoma (ACC) is a rare tumor with an estimated incidence of 0.5–2 cases per 1 million people per year and it has a poor prognosis with a 5-year survival rate below 15 % in advanced metastatic stages [1]. Treatment options in advanced, metastatic stages are limited, since the results of cytotoxic chemotherapy are mostly poor and radiotherapy is usually ineffective, as well [1–3]. Based on the results of the recent FIRM-ACT trial involving the two most widely used cytotoxic regimens, the median duration of overall survival has been 14.8 months in the EDP-mitotane (etoposide–doxorubicin–cisplatin + mitotane), and 12 months in the

streptozotocin–mitotane groups [4]. The only adrenal specific drug that is currently licensed for the treatment of adrenocortical carcinoma is mitotane (*o,p'*-dichlorodiphenyldichloroethane (*o,p'*-DDD)). Mitotane has adrenolytic activity, and is used as a monotherapy, in combination with cytotoxic chemotherapy or as an adjuvant therapy after complete surgical resection [5]. The major drawback of mitotane is its toxicity, the narrow therapeutic window and frequent side effects (gastrointestinal, neurological, etc.) [6]. Given the high mortality and aggressiveness of ACC, more effective and specific treatment options would be needed. Intensive efforts are going on for finding novel therapeutic regimens, however, no breakthrough has been reported yet. Studies on the pathogenesis of ACC are therefore of pivotal relevance for establishing novel therapeutic targets.

In our previous meta-analysis study of adrenocortical tumor genomics data, retinoic acid signaling via retinoid X receptor was established as an important pathogenic pathway in ACC. These significant retinoic acid-dependent pathways were: cholesterol and lipid metabolism (RXR/LXR and RXR/PPARG signaling) and the bacterial lipopolysaccharide (LPS) recognition via Toll-like receptor 4 (TLR4) [7]. Moreover, ACC was associated with diminished retinoic acid production [7]. In a previous *in vitro* study on the NCI-H295R adrenocortical cell line, 9-*cis* retinoic acid (9-*cis*RA) was able to reduce DNA synthesis [8].

Retinoids are natural and synthetic derivatives of vitamin A, which play fundamental roles in the regulation of cell growth, differentiation, and death. Retinoids act through two distinct nuclear receptors, the retinoic acid receptors (RAR α , RAR β , RAR γ) and the retinoic X receptors (RXR α , RXR β , RXR γ), which are ligand-inducible transcription factors [9, 10]. RARs bind both all-*trans* retinoic acid (ATRA) and 9-*cis* retinoic acid while RXRs bind only 9-*cis*RA [10].

Several studies demonstrated the antiproliferative effect of 9-*cis*RA treatment in different cancer types *in vitro* and in animal models (e.g., hepatocellular carcinoma [11, 12], breast cancer [13, 14]). 9-*cis*RA is used for the therapy of Kaposi's sarcoma [15] and its antitumoral effect was also investigated in further clinical trials [16]. The purpose of the present study was to examine the *in vitro* effects of 9-*cis*RA treatment on cell death, hormone secretion, and gene expression in the NCI-H295R cell line. Moreover, we applied systems biology approaches (pathway and network analysis) for deciphering the molecular mechanisms involved in 9-*cis*RA action. To confirm our findings in an *in vivo* model, a pilot xenograft study has also been performed. We hypothesized that 9-*cis*RA might inhibit hormone secretion and cell proliferation in the NCI-H295R cell line, and induce gene expression changes.

Materials and methods

Cell culture and treatments

Human adrenocortical NCI-H295R cell line was obtained from the American Type Culture Collection (Manassas, VA, USA). Cells were cultured in Dulbecco's modified Eagle's medium/Nutrient Mixture F-12 Ham (DMEM: F12) supplemented with 6.25 ng/ml selenium (Sigma-Aldrich Chemical Co.), 0.00535 mg/ml linoleic acid, 0.00625 mg/ml insulin, 0.00625 mg/ml transferrin (Sigma-Aldrich Chemical Co.), 1.25 mg/ml bovine serum albumin and adjusted to a final concentration of 1 % HEPES, 1 % Penicillin/Streptomycin (Sigma-Aldrich Chemical Co., St. Louis, MO, USA), 2.5 % Nu-Serum (BD Biosciences, San Jose, CA, USA) and 2.5 % L-glutamine (Sigma-Aldrich Chemical Co.) at 37 °C in a humidified 5 % CO₂ atmosphere. The medium was changed two to three times a week and subcultured every 7 days.

NCI-H295R cells were treated for 24, 48 and 72 h with 9-*cis*RA (Sigma-Aldrich Chemical Co.) at final concentrations of 10⁻⁵ M; 2.5 × 10⁻⁵ M; 5 × 10⁻⁵ M; 7.5 × 10⁻⁵ M and 10⁻⁴ M dissolved in absolute ethanol. The control groups were treated with the same amount of ethanol.

Cell viability analysis

Flow cytometry has been used for the analysis of cell viability based on our previous study of mitotane on NCI-H295R cells showing a very good correlation of our flow cytometry protocol and the MTT (3-(4,5-dimethylthiazol-2-yl)-2,5-diphenyl-tetrazolium bromide) assay [17]. NCI-H295R cells were plated at a density of 1.5 × 10⁵ cells per well into 12-well microplates in complete culture medium. After 48 h incubation, cells were treated with 9-*cis*RA at 10⁻⁵ M; 2.5 × 10⁻⁵ M; 5 × 10⁻⁵ M; 7.5 × 10⁻⁵ M and 10⁻⁴ M final concentrations and incubated for 24, 48, and 72 h. The control group was treated with an equivalent amount of ethanol. Cells were trypsinized, collected in PBS, and measured with a FACSCalibur (BD Biosciences) cytometer. Data were analyzed using CellQuest Pro™ 90 software (BD Biosciences). At least 10,000 events were collected. Live and dead cells were discriminated on the basis of cell size (forward scatter, FSC) and cell granularity (side scatter, SSC) [18].

Steroid hormone secretion analysis

Dehydroepiandrosterone (DHEA), cortisol, and aldosterone concentrations were measured in cell culture supernatants. DHEA was measured by radioimmunoassay using DHEA RIA kit (Immunotech, Beckman Coulter Inc., Prague, Czech Republic) by RIA-mat280 (DiaSorin, Stillwater, MN, USA). Cortisol was determined on Cobas e411 (Roche

Diagnostics, Basel, Switzerland) by the Roche Cobas Cortisol electrochemiluminescence immunoassay. Aldosterone was measured using the Aldosterone Radioimmunoassay Kit (DiaSorin) measured with RIA-mat280 (DiaSorin) according to the instructions of the manufacturer.

RNA isolation

Total RNA was isolated from 2×10^6 9-*cis*RA treated (2.5×10^{-5} M; 5×10^{-5} M; 7.5×10^{-5} M for 24 h) and control NCI-H295R cells with Qiagen miRNeasy Mini Kit and RNase-Free DNase Set according to the manufacturer's protocol (Qiagen, Hilden, Germany). RNA concentration was measured by NanoDrop 1000 Spectrophotometer (Thermo Fisher Scientific Inc., Waltham, MA, USA) and RNA integrity was determined by an Agilent 2100 Bioanalyzer System (Agilent Technologies Inc., Santa Clara, CA, USA). Samples with an RNA integrity number (RIN) above 8.0 were used for further analysis. RNA was stored at -80°C until use.

Messenger RNA expression profiling

Gene expression profiling was performed on 12 samples (3–3 samples of 2.5×10^{-5} M; 5×10^{-5} M, 7.5×10^{-5} M 9-*cis*RA treated NCI-H295R cells and 3 control samples at 24 h) using single-color array method by $4 \times 44\text{K}$ Agilent Whole Genome Microarray slides (Agilent Technologies Inc.).

Total RNA (200 ng) was labeled and amplified using the Low Input Quick Amp Labeling Kit according to the instructions of the manufacturer. Labeled RNA was purified and hybridized to Agilent Whole Human Genome Microarray slides, according to the manufacturer's protocol. After washing, array scanning and feature extraction was performed with default scenario by Agilent DNA Microarray Scanner and Feature Extraction Software 9.5.3. Total gene signal normalization at the 75th percentile of raw signal values and baseline transformation at the median of all samples was performed by GeneSpring software 10.1 following Agilent's recommendation. Genes were filtered by flag values (100 % of samples are present or marginal in at least one group) and raw data (expression is higher than 20 percentile in the 100 % of samples in at least one group). Fold change filter was set to twofold between 9-*cis*RA-treated groups versus control cells and adenoma versus carcinoma in the public available datasets (Agilent Technologies Inc.).

Microarray datasets from previously published studies

To compare 9-*cis*RA-caused gene expression changes and results of previously published adrenocortical adenoma

(ACA) and ACC microarray studies, whole-genome raw mRNA expression data of 154 tumor (87 ACA and 67 ACC) samples from Gene Expression Omnibus (GEO, <http://www.ncbi.nlm.nih.gov/geo>) and ArrayExpress (<http://www.ebi.ac.uk>) were obtained [19–21], reclassified and reanalyzed. Further significant gene sets from studies where raw gene expression data were unavailable have been collected from OncoPrint Research (<http://www.oncoprint.org>) [22] and seven papers found by literature search (PubMed, <http://www.ncbi.nlm.nih.gov/pubmed>) [23–28], which included 182 ACA and 91 ACC samples. Altogether, microarray data from 269 ACA and 158 ACC samples were available.

Pathway analysis

Pathway analysis was performed by Ingenuity Pathway Analysis (IPA) software (Ingenuity Systems, www.ingenuity.com; Redwood City, CA, USA). All gene sets retrieved from the statistical analysis were loaded into the IPA software.

Gene expression network

IPA was also used for the generation of 35 member molecular networks. We have searched for common significant gene expression changes between at least two independent 9-*cis*RA treatments in the NCI-H295R cell line and at least two ACA versus ACC comparisons from previously published microarray studies. Scale-free distribution of degree was investigated by linear regression following the logarithmic transmission of values. Ten percent of nodes with the highest number of links were identified as hubs in the network [29]. For network hierarchization, vertex sort algorithm [30] was used, and for the identification of network motifs, mFinder software [31] was used. Network analysis was performed by our own software written in Java program language.

Quantitative reverse-transcription PCR

To select the optimal treatment time, two known RXR target genes, *ABCA1* and *ABCG1* [32], were selected for the examination of 9-*cis*RA-induced gene expression changes by quantitative real-time reverse-transcription polymerase chain reaction (qRT-PCR) using TaqMan gene expression assays (Applied Biosystems): *ABCA1* (Hs01059118_m1), *ABCG1* (Hs00245154_m1). *ZNF625* (Hs00377010_m1) was used as a housekeeping gene, based on our previous study [17]. Total RNA (10 ng) was reverse transcribed using High-Capacity cDNA Reverse Transcription Kit (Applied Biosystems, Foster City, CA, USA). Quantitative RT-PCR was performed by TaqMan Fast Universal PCR Master Mix (2x)

(Applied Biosystems) on a 7500 Fast Real-Time PCR System (Applied Biosystems) according to the manufacturer's protocol. Gene expression differences between the investigated groups were calculated using the ddCT method [33] according to the manufacturer's instructions (SDS Program, Applied Biosystems). Calibration curves have also been taken [34] that showed 100 % efficiency of gene amplification with the industrial primer pairs and reaction conditions used in our analysis. Samples were run in triplicate.

After mRNA expression profiling and pathway analysis, eight genes were selected for validation. TaqMan Gene Expression Assays (Applied Biosystems) were used as follows: *CCNE2* (Hs00180319_m1), *GADD45A* (Hs00169255_m1), *HSD3B1* (Hs00426435_m1), *HSD3B2* (Hs00605123_m1), *HMGCR* (Hs00168352_m1), *IL1R2* (Hs01030384_m1), *MAP2K6* (Hs00992389_m1), *UHRF1* (Hs01086727_m1). To identify the most appropriate housekeeping gene in our analysis, we have used the criteria established by Cheng et al. [35]: (1) raw intensity value is higher than 20 % in at least 80 % of samples in each group, (2) Coefficient of variation is lower than 0.3, and (3) fold change is lower than 1.2. Based on this method, *R3HDM2* (Hs00248196_m1) was used as a housekeeping gene for the validation [35]. Gene expression differences were calculated as described above.

Xenograft model

For the xenograft model, six male nude mice aged 3 months were inoculated subcutaneously with 6×10^6 cells/100 μ l PBS NCI-H295R cell suspension [36, 37]. Treatment was started as the solid tumor reached 5 mm mean diameter (33 days after NCI-H295R incubation). 3–3 mice were injected intraperitoneally with 10 mg/kg/day 9-*cis*RA (Carbosynth, Compton, UK) or vehicle (DMSO diluted in PBS) for 28 days [38]. Tumors were measured twice a week by the same investigator using a digital caliper. Tumor volume was calculated by the following formula: V (mm³) = (width² (mm) \times length (mm) \times π)/6. Tumor volume was normalized to the first measurement in each case (V_t/V_0). On day 29, mice were killed by cervical dislocation in ether anesthesia. Tumors were removed, their weight was measured, and they were fixed in formalin. All animal experiments were conducted according to the ethical standards of the Animal Health Care and Control Institute, Csongrád County, Hungary, permit No. XVI/03047-2/2008.

Histology and Ki67 immunostaining

Ten-micrometer sections of formalin-fixed paraffin-embedded tumors from nude mice were dewaxed with xylene and ethanol, and then processed either for hematoxylin and eosin (H&E) staining or Ki67 immunostaining. For antigen retrieval, sections were microwaved in 10 mM citrate buffer

(pH 6) for 20 min. Next, the slides were blocked with 5 % bovine serum albumin dissolved in PBS for 30 min. Ki67 primary antibody (Cat. No. M7240, DakoCytomation, Glostrup, Denmark) was diluted in 1 % BSA in a ratio of 1:100, and applied overnight at 4 °C. The next day, the slides were washed three times with PBS and incubated with secondary antibody (anti-mouse immunoglobulins/HRP Cat. No. P0447, DakoCytomation) for 30 min. After washing, signals were developed using DAB + Substrate Chromogen System (Dako). Slides were counterstained with hematoxylin. The Ki67 index was obtained by counting immunopositive cells of 3–3 random field from each tumor. Pictures were taken with a Zeiss Axioskop 2 Plus light microscope (Zeiss, Oberkochen, Germany) with an Olympus DP50 camera (Olympus, Tokyo, Japan).

Statistical analysis

Statistical analysis of viability, hormone secretion, and qRT-PCR data was performed by Microsoft Office Excel 2010 (Microsoft Corp., Redmond, WA, USA), and Statistica 8.0 (StatSoft Inc., Tulsa, OK, USA) software. Viability and hormone secretion data were subjected to two-way ANOVA and qRT-PCR data were subjected to one-way ANOVA each followed by Tukey's post hoc test.

Statistical analysis of microarray data was performed by GeneSpring 10.1 (Agilent Technologies Inc.) software. Identification of differently expressed genes between 9-*cis*RA treated groups and control cells were carried out by one-way ANOVA, followed by Tukey's Honestly Significant Difference post hoc test. For the identification of differently expressed genes between ACA and ACC groups, unpaired Student's *t* test was used. Each test was followed Benjamini–Hochberg false discovery rate (FDR < 0.25) calculation.

To correlate gene expression changes with the concentration of 9-*cis*RA, Spearman correlation was used (*p* value < 0.05, $R^2 > 0.7$).

For in vivo studies, the Mann–Whitney *U* test was applied to reveal significances between control and 9-*cis* retinoic acid-treated groups.

Results

Selection of optimal treatment time and concentration

To select the optimal treatment time and concentrations, live–dead cell ratio, steroid hormone levels, and RXR target gene expression changes were measured.

A significant decrease in the living cell population was observed after 24 h at 10^{-4} M 9-*cis*RA treatment. After 48 and 72 h treatments at 7.5×10^{-5} M 9-*cis*RA

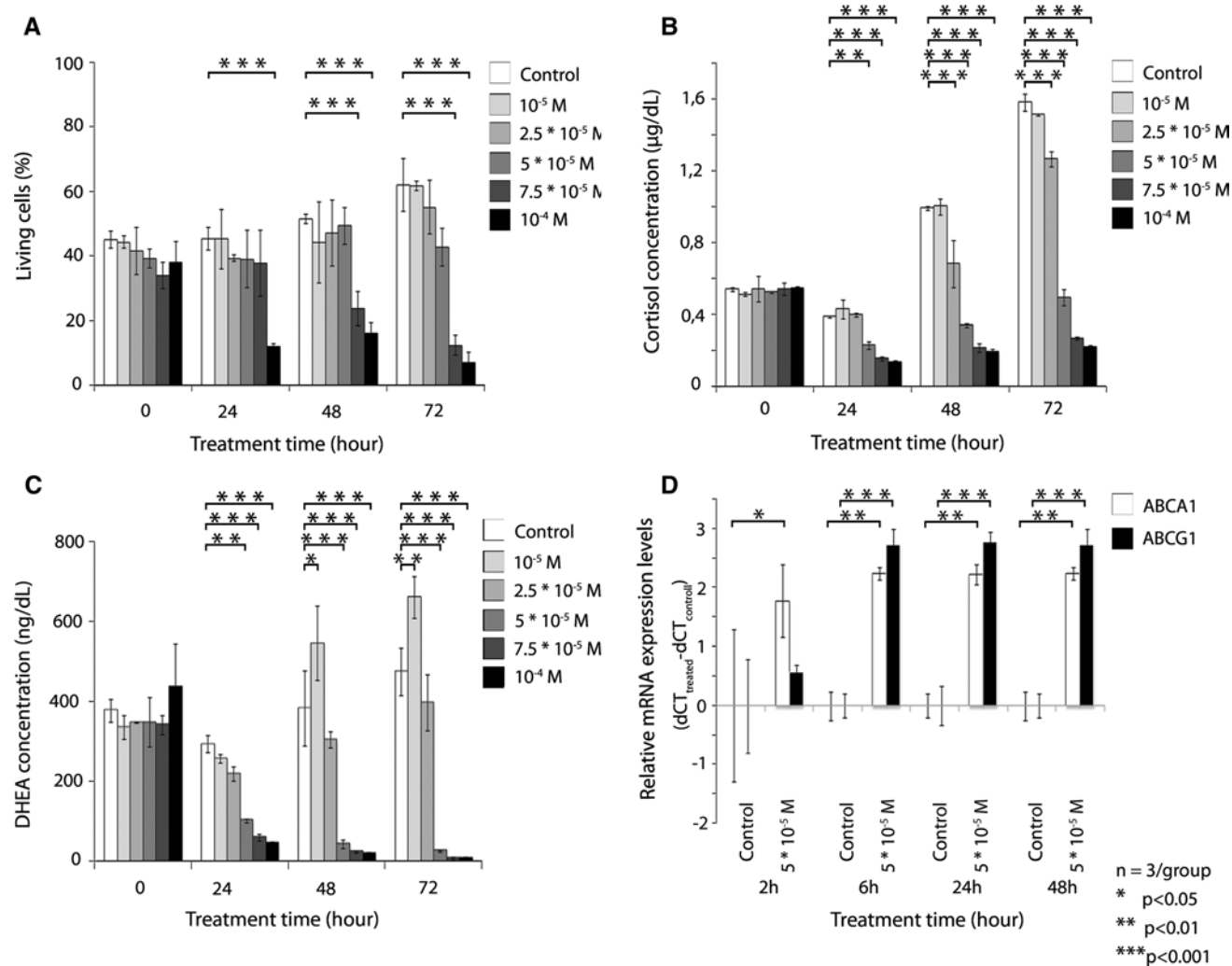


Fig. 1 Effects of 9-*cis*RA on cell viability assay (a), on cortisol (b), and DHEA (c) secretion in five different concentrations and three different treatment periods and the relative mRNA expression level of *ABCA1* and *ABCG1* RXR target genes relative to the housekeeping

gene *ZNF625* in one concentration and four different treatment times (d) in NCI-H295R cells ($n = 3$, mean \pm SD, * $p < 0.05$, ** $p < 0.01$, *** $p < 0.001$ relative to control)

concentration, the proportion of living cells was also significantly reduced relative to the untreated control, but at lower concentrations, no significant cell death occurred (Fig. 1a). Significant reduction of cell viability has been observed between the 0 and 72 h time points at the 7.5×10^{-5} M 9-*cis*RA concentration and at all time points at 10^{-4} M (Supplementary Figure 1).

Since NCI-H295R cells secrete several steroid hormones (i.e., glucocorticoids, mineralocorticoids, and adrenal androgens [39]), the measurement of cortisol, DHEA, and aldosterone levels was performed in both control and 9-*cis*RA-treated cells after 24, 48, and 72 h. As shown in Fig. 1b, c, both cortisol and DHEA levels significantly decreased after 24 h in a concentration-dependent manner. Aldosterone concentration was under RIA detection level

(<0.1 ng/dl) (data not shown). Whereas time-dependence of DHEA secretion inhibition by 9-*cis*RA at 5×10^{-5} M and 7.5×10^{-5} M has been noted (Supplementary Figure 1), cortisol levels could not be clearly associated with treatment time (data not shown).

The expression of known RXR target genes: *ATP-binding cassette, sub-family A, member 1* (*ABCA1*) and *ATP-binding cassette, sub-family G, member 1* (*ABCG1*) after 6 h treatment at 5×10^{-5} M 9-*cis*RA concentration reached the maximal relative mRNA expression level. The significant overexpression of *ABCA1* and *ABCG1* has been observed from 2- and from 6-h treatment onward, respectively (Fig. 1d).

We have selected the 24-h treatment time and 9-*cis*RA concentrations of 2.5×10^{-5} M; 5×10^{-5} M and

7.5×10^{-5} M to investigate gene expression changes by microarray analysis. We have not observed a significant reduction in cell viability at our selected 24-h treatment time at any of these concentrations.

Microarray analysis

Altogether, 12 samples have been subjected to microarray analysis: 3–3 samples of control and 2.5×10^{-5} M; 5×10^{-5} M; 7.5×10^{-5} M 9-*cis*RA-treated NCI-H295R cultures at 24 h. All results are available at Gene Expression Omnibus (<http://www.ncbi.nlm.nih.gov/geo>) under Accession Number: GSE43090.

We have identified 699, 2,320, and 2,303 significantly differentially expressed genes ($p < 0.05$) by the statistical analysis of microarray data between control and the 2.5×10^{-5} M, 5×10^{-5} M and 7.5×10^{-5} M 9-*cis*RA-treated cell cultures, respectively (Supplementary Table 1, and Supplementary Figure 2).

To identify genes that might be relevant in the potential antitumoral activity of 9-*cis*RA in adrenocortical cancer, we have compared the 9-*cis*RA-induced gene expression changes in the NCI-H295R cell line with established, already published gene expression pattern differences between benign and malignant adrenocortical tumors. We have searched for common, but inversely associated significantly differentially expressed genes between 9-*cis*RA-treated NCI-H295R cells and the adenoma-carcinoma comparison. We hypothesized that the potential antitumoral effects of 9-*cis*RA might be represented by genes that are underexpressed in ACC relative to adenomas, but whose expression is increased by 9-*cis*RA in the NCI-H295R cells, and vice versa. Thus, 9-*cis*RA treatment might “reverse” some gene expression changes characteristic for malignant tumors.

We detected 246 genes that were common in at least two comparisons of control and 9-*cis*RA treated groups and in at least two former ACA and ACC microarray studies [19–28] (Supplementary Table 2). Three genes were common in at least two 9-*cis* retinoic acid treated-control comparisons and six ACA versus ACC microarray studies: *ATP-binding cassette, sub-family C (CFTR/MRP), member 3 (ABCC3)*, *aldehyde dehydrogenase 1 family, member A1 (ALDH1A1)*, *sema domain, transmembrane domain (TM), and cytoplasmic domain, (semaphorin) 6A (SEMA6A)*.

Pathway analysis

Pathway analysis of the significant gene lists revealed 21 canonical pathways in at least two comparisons of control and 9-*cis*RA-treated groups and in at least two ACA and ACC microarray studies [19–28]. These included steroid hormone metabolism (C21-Steroid Hormone Metabolism

(Fig. 2), retinoic acid signaling (LPS/IL-2 Mediated Inhibition of RXR Function, LXR/RXR Activation, PXR/RXR Activation) (Fig. 3), cell-cycle regulation (ATM Signaling, GADD45 Signaling) (Fig. 4), (Aryl Hydrocarbon Receptor Signaling, Cyclins and Cell-Cycle Regulation and Estrogen-mediated S-phase Entry) (Supplementary Figure 3) and immune regulation (p38 MAPK Signaling, MIF Regulation of Innate Immunity) (Supplementary Figure 4) (Supplementary Table 3).

Gene expression networks

For the IPA network analysis, common genes in at least two comparisons of control and 9-*cis*RA-treated groups and in at least two ACA and ACC microarray studies [19–28] were used. The top two networks were merged for the exploration of nodes with the highest number of connections. The merged networks were scale-free ($R^2 = 0.755$, power parameter -0.844) and contained 72 nodes. Six genes (10 % of highest degree nodes) were marked as hubs: *cyclin-dependent kinase 1 (CDK1)*, *cyclin A (CCNA)*, *E2F transcription factor (E2F)*, *mitogen-activated protein kinase (ERK1/2)*, *nuclear factor kappa-B (NFKB)*, *retinoblastoma (RB)*. Following the hierarchization process, nodes based on the direction of their edges were categorized into top, core, and bottom layers. As the top layer of the investigated network contained two 9-*cis*RA receptor transcription factor complexes (LXR-RXR and NCOR-LXR-RXR), we concluded that the whole network is under 9-*cis*RA regulation. With the mFinder software, we have identified four significantly enriched motif types that contained 118 3-node motifs. The majority of these motifs were feed-forward loop (FFL), among these three FFL crossed each layer (Supplementary Figure 5).

Gene validation by qRT-PCR

Based on the microarray data and the pathway-analysis results, eight genes have been selected for further qRT-PCR validation and sample size extension. All eight genes were successfully validated: *cyclin E2 (CCNE2)*, *growth arrest and DNA-damage-inducible, alpha (GADD45A)*, *hydroxy-delta-5-steroid dehydrogenase, 3 beta- and steroid delta-isomerase 1 (HSD3B1)*, *hydroxy-delta-5-steroid dehydrogenase, 3 beta- and steroid delta-isomerase 2 (HSD3B2)*, *3-hydroxy-3-methylglutaryl-CoA reductase (HMGCR)*, *interleukin 1 receptor, type II (IL1R2)*, *mitogen-activated protein kinase kinase 6 (MAP2K6)*, *ubiquitin-like with PHD and ring finger domains 1 (UHRF1)* (Fig. 5). By Spearman correlation, all validated gene expression changes (except for *IL1R2*) correlated significantly with 9-*cis*RA concentration (Supplementary Figure 6).

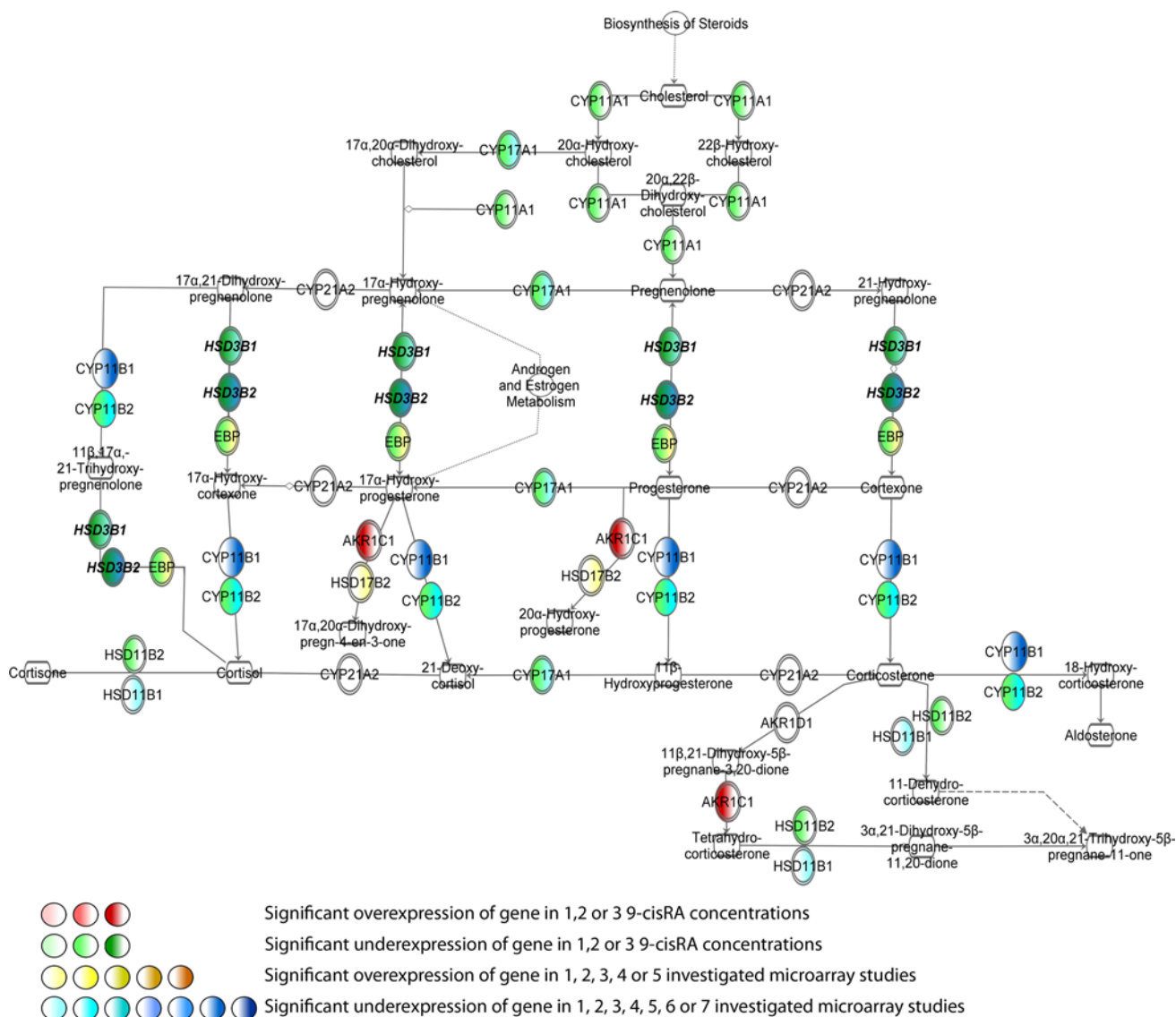


Fig. 2 Pathways with related gene expression patterns involved in the steroid hormone metabolism after 9-cisRA treatment in NCI-H295R cells (left sides of circular symbols representing gene expression) and

investigated microarray studies in ACC (right sides of circular symbols representing gene expression)

Xenograft model

Since there was no data on the dose of 9-cisRA for in vivo adrenocortical tumor xenograft models, we used the effective 9-cisRA dose (10 mg/kg) reported in breast cancer xenografts [38]. The growth of H295R-derived tumors has been identical between the control and 9-cisRA-treated animals until day 15, but thereafter the tumors in the 9-cisRA-treated animals have grown to a lesser extent than the controls (Fig. 6a). At the end of treatment (day 28), a tumor volume normalized to the initial size increased 10.1 times in control animals versus 5.4 times in the mice treated with 9-cis retinoic

acid (Fig. 6b). The weight of the excised tumors confirmed these results, as an average of 2.7 and 1.4 g was measured for control and retinoic acid-treated tumors, respectively (Fig. 6c). Due to the small number of animals included, these differences did not reach statistical significance, but the tendency seems to be clear-cut. Tumors of 9-cis retinoic acid-treated animals were more differentiated than those of control ones as observed on hematoxylin and eosin (H&E)-stained sections (Fig. 6d). Note the cord-like arrangement of the tumor cells, which reminds one of the normal structure of adrenal cortex in 9-cis retinoic acid-treated tumors. Dividing tumor cells were seen in both cases, but with a higher number in the

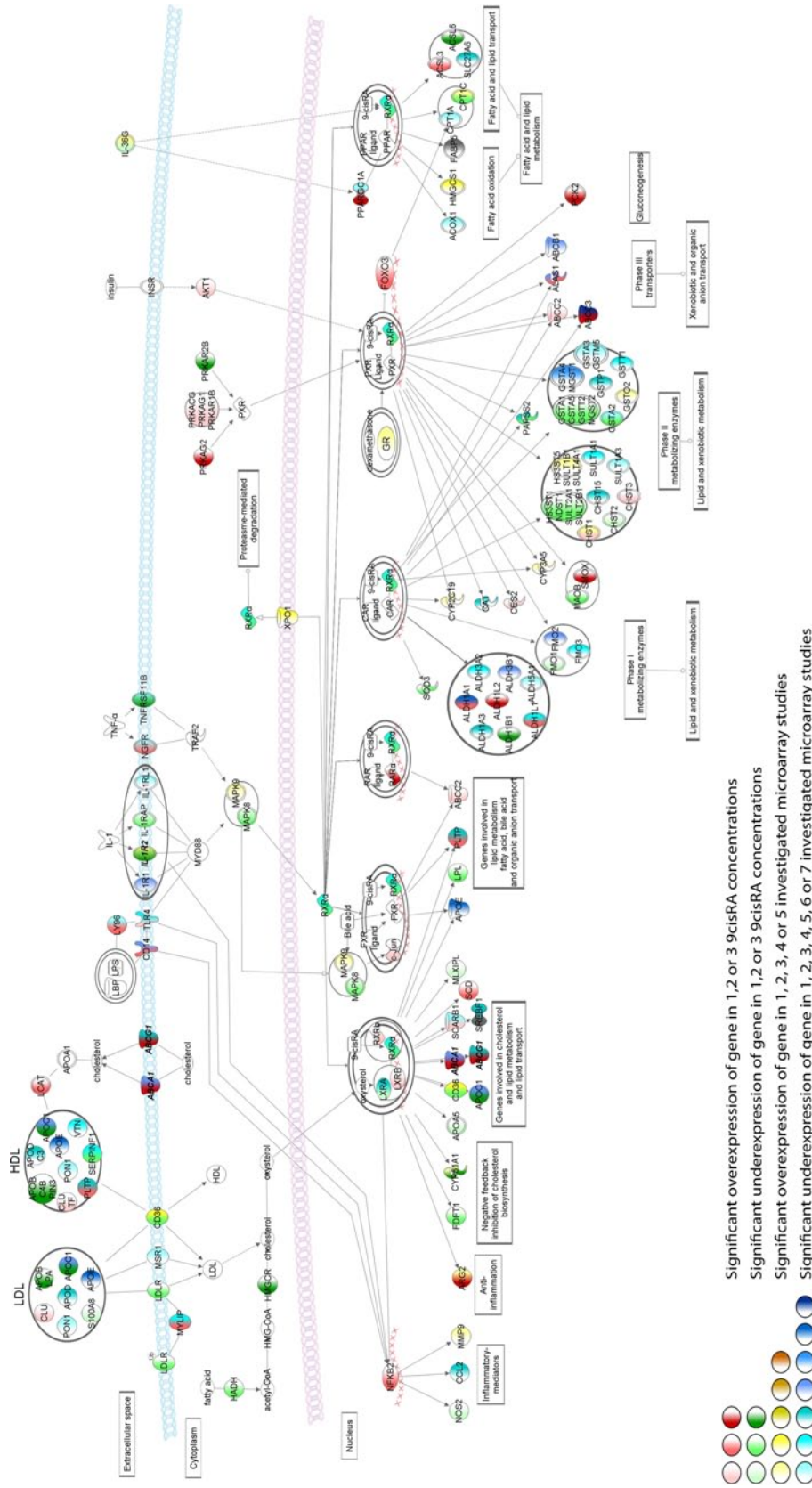


Fig. 3 Pathways with related gene expression patterns involved in retinoic acid signaling after 9-cisRA treatment in NCI-H295R cells (left sides of circular symbols representing gene expression) and investigated microarray studies in ACC (right sides of circular symbols representing gene expression)

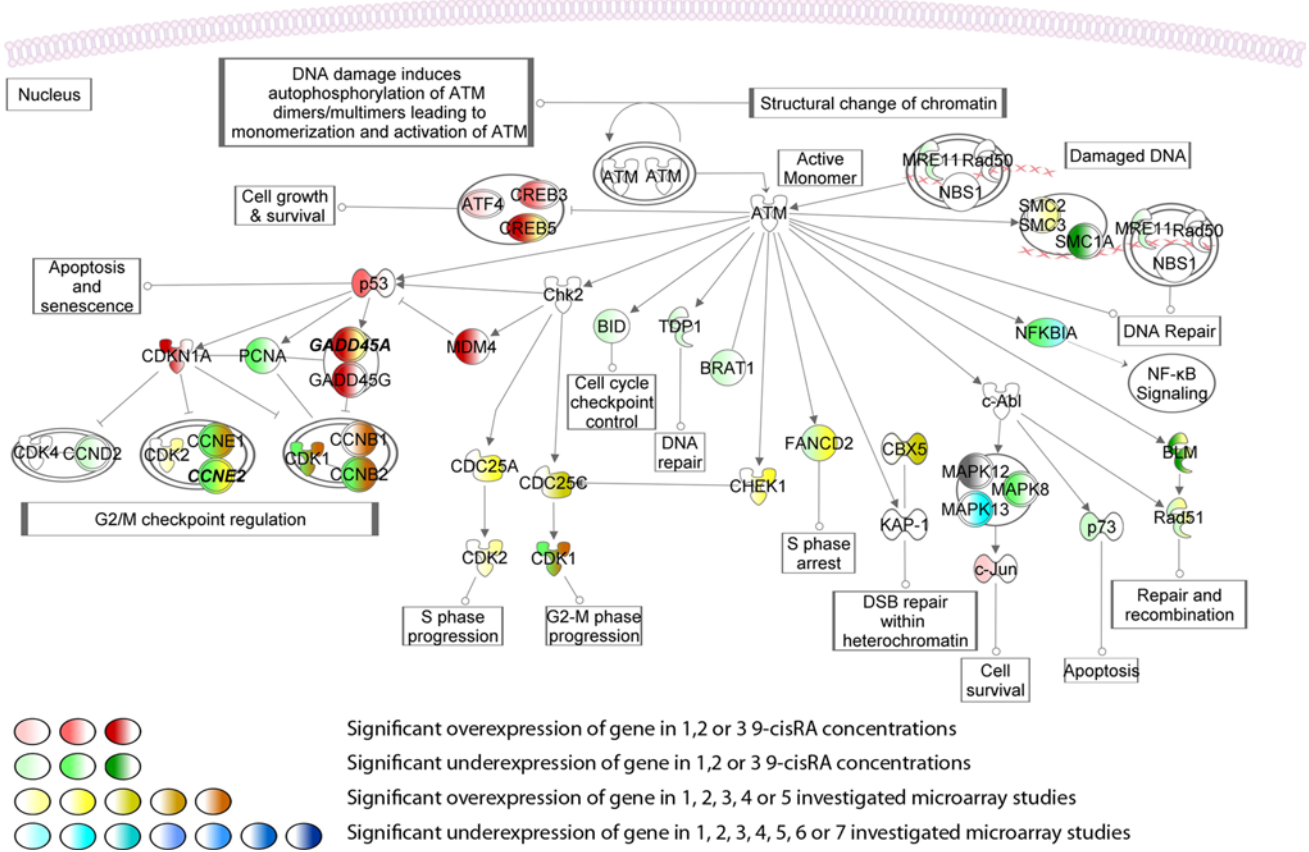
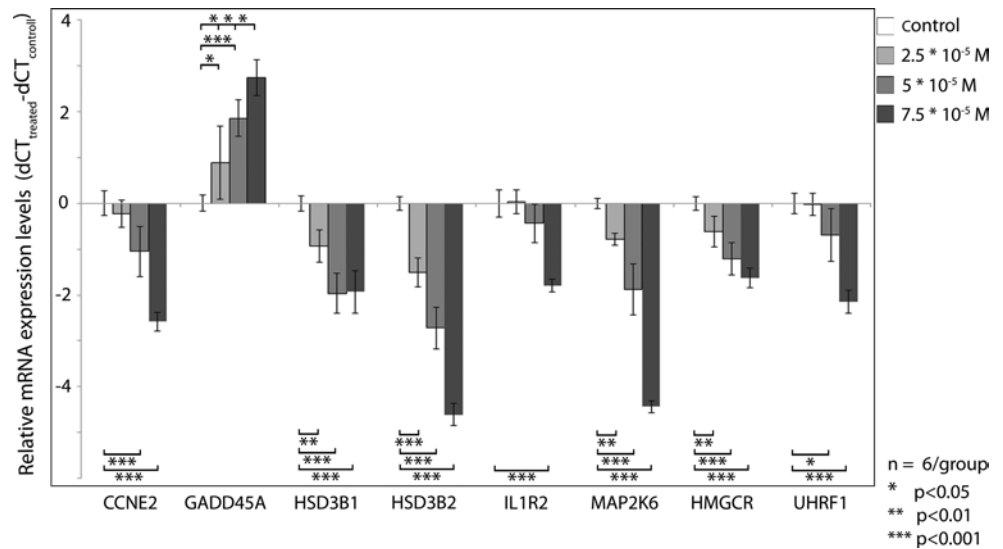


Fig. 4 Pathways with related gene expression patterns involved in cells cycle regulation (Ataxia Telangiectasia Mutated (ATM) Signaling, Growth arrest and DNA-damage-inducible (GADD45) Signaling) after 9-*cis*RA treatment in NCI-H295R cells (left sides of circular

symbols representing gene expression) and investigated microarray studies in ACC (right sides of circular symbols representing gene expression)

Fig. 5 Results of qRT-PCR validation of eight selected genes relative to the housekeeping gene *R3HDM2*. Results are represented by ddCT (cycle threshold) compared to the control after three different 9-*cis*RA treatment in concentrations at 24-h treatment time (mean ± SD, **p* < 0.05; ***p* < 0.01, ****p* < 0.001 relative to control *n* = 6)



control samples (Fig. 6d, arrows). Ki67 immunostaining revealed a significantly elevated number of proliferating tumor cells in the control sections compared to treated

ones (130.8 vs. 50.4, *p* < 0.001) reflecting the effectiveness of 9-*cis* retinoic acid in inhibiting tumor cell proliferation (Fig. 6d, e).

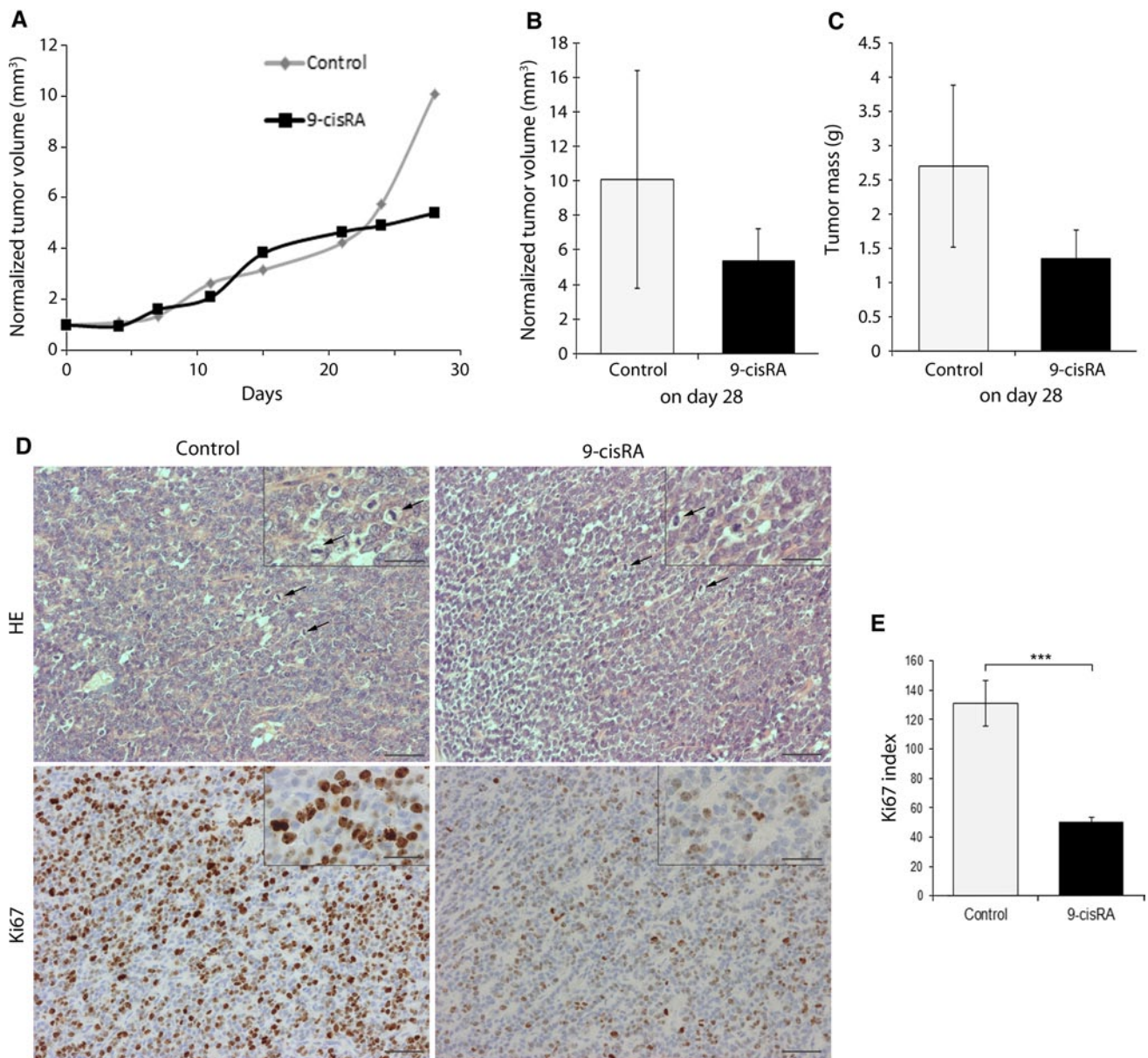


Fig. 6 Results of the in vivo xenograft studies. **a** Growth curve of tumors in control and 9-cisRA-treated mice. **b** Diagrams showing the normalized tumor volume at the end of treatment (day 28) in control and 9-cis retinoic acid-treated (9-cisRA) animals. Values are expressed as mean \pm SE. **c** Differences in tumor weight on the day 28 of 9-cis retinoic acid treatment between control animals and mice exposed to 9-cisRA. Results are expressed as mean \pm SE. **d** Representative pictures of H&E staining and Ki67 immunoreaction on

tumors from control and 9-cis retinoic acid-treated nude mice. Note the alteration in histology of 9-cisRA-treated tumors, where tumor cells are arranged in cords, reminding one of the structure of normal adrenal cortex. Arrows point to dividing cells. Scale bars represent 50 and 25 μ m for insets. **e** Diagrams displaying Ki67 index obtained by counting immunopositive cells on sections from control and 9-cisRA tumors. Results are expressed as mean \pm SE, *** p < 0.001

Discussion

We have found that 9-cisRA treatment significantly decreased cell viability and steroid hormone secretion in a concentration- and time-dependent manner. The minimal significant cytotoxic concentration was 7.5×10^{-5} M. This is similar to the cytotoxic concentrations of 9-cisRA on human hepatocellular carcinoma cells in vitro and in rat models [11].

The activity of 9-cisRA in our pilot xenograft model demonstrates the in vivo antitumoral cytotoxic activity of this agent, as well, and might pave the way for further larger-scale studies.

To identify the potential benefits of the 9-cisRA treatment in adrenocortical carcinoma, we searched for gene expression changes between ACA and ACC [19–28] of inverse direction as that induced by 9-cisRA treatment.

The pathway analysis of these comparisons revealed four major pathways: (1) steroid hormone secretion, (2) retinoic acid signaling, (3) cell-cycle damage, and (4) changes of immune response. We have selected eight genes representing these pathways, and all of these have been successfully validated by qRT-PCR. The two known 9-*cis*RA target genes (*ABCA1* and *ABCG1*) validated for treatment optimization belong to the retinoic acid pathway, thus the number of all validated genes is ten. Below we describe the major features of these pathways and their potential relevance. All important results have been summarized in Table 1.

Steroid hormone metabolism

9-*cis*RA treatment significantly decreased cortisol and DHEA concentration in a concentration-dependent manner. With microarray analysis, we have observed the 9-*cis*RA-induced underexpression of several enzymes involved in steroid hormone biosynthesis and metabolism: *cytochrome P450 side chain cleavage enzyme (sc)* (*CYP11A1*), *steroid 11-beta-monooxygenase (CYP11B2)*, *steroid 17-alpha-monooxygenase (CYP17A1)*, *emopamil binding protein (EBP)*, *hydroxysteroid (11-beta) dehydrogenase 2 (HSD11B2)*, *HSD3B1*, *HSD3B2*. We have validated the 9-*cis*RA-induced underexpression of *HSD3B1* and *HSD3B2* by qRT-PCR.

HSD3B1 and *HSD3B2* convert pregnenolone/17 α -hydroxypregnenolone to progesterone/17 α -hydroxyprogesterone. *HSD3B1* gene underexpression was found in one of the analyzed microarray studies in ACC [26]. Despite having validated the 9-*cis*RA-induced *HSD3B1* underexpression in the NCI-H295R cell line, it should be mentioned that this enzyme is mainly expressed extra-adrenally [40] and the relevance of its 9-*cis*RA-induced underexpression is thus unclear. Overexpression of *HSD3B2* gene was reported in ACA compared to normal adrenal [41] and we found underexpression in five microarray studies in ACC [19, 20, 22, 23, 27].

The inhibition of hormone secretion by 9-*cis*RA on NCI-H295R cells thus seems to be mediated at least in part at the level of gene expression. Other retinoids including ATRA also seem to decrease the expression of some enzymes involved in steroid hormone biosynthesis (e.g., ATRA inhibited *HSD3B* expression in mouse Leydig cells [42], and corticosterone production and cell proliferation in Y1 mouse adrenocortical cells [43]).

Retinoic acid signaling

Retinoids play crucial roles in the regulation of cell growth, differentiation, and death. Their biological function is mediated via two types of receptors: the retinoic acid receptors (*RAR α* , *RAR β* , *RAR γ*) and the retinoic X receptors (*RXR α* ,

RXR β , *RXR γ*). *RXR* is specific for 9-*cis*RA, whereas *RAR* can bind both 9-*cis*RA and ATRA. *RXR* may heterodimerize with other nuclear receptors including liver X receptor (*LXR*), farnesoid X receptor (*FXR*), *RAR*, constitutive androstane receptor (*CAR*), pregnane X receptor (*PXR*), and peroxisome proliferator-activated receptor (*PPAR*) [8, 10].

We have observed several 9-*cis*RA-induced gene expression changes in the permissive *RXR* partners (*LXR*, *FXR*, *PXR*, *PPAR*). *LXRs* participate in adrenal cholesterol metabolism and influence steroid hormone production [44]. The adrenal gland expresses liver X receptor *LXRA* and *LXRB*, and their expression has been induced by 9-*cis*RA treatment. *LXRA* gene underexpression was found in ACC in three studies [19–21]. *ABCA1* and *ABCG1* genes were significantly overexpressed by 9-*cis*RA treatment, and successfully validated by qRT-PCR. *ABCA1* and *ABCG1* were significantly underexpressed in ACC in four and three studies, respectively (*ABCA1*: [19–21, 27] and *ABCG1*: [19–21]), and 9-*cis*RA treatment produced a gene expression alteration inverse to that observed in the ACA–ACC comparison. Although not included in the pathway, it should be mentioned that we have validated the 9-*cis*RA induced underexpression of *HMGCR* gene that is the rate-limiting step in cholesterol biosynthesis. This observation underlines the potential involvement of cholesterol metabolism in 9-*cis*RA action.

CAR and *PXR* are closely associated with each other and involved in the regulation of cell growth, apoptosis, tumorigenesis, energy metabolism, and induction of drug-metabolizing enzymes [45]. Activation of *CAR* and *PXR* receptors induces the *ABCC3* gene, and *CAR* induces the *ALDH1A1* and *ALDH1L1* genes [46]. *ALDH1A1* catalyzes the rate-limiting second oxidative step of retinoic acid biosynthesis. We have found decreased *ALDH1A1* mRNA expression in ACC compared to ACA in six microarray studies [19, 20, 23, 25–27], contrary to its increased expression after 9-*cis*RA treatment. Two studies have validated the underexpression of *ALDH1A1* in ACC by qRT-PCR [23, 25].

PPARG regulates the expression of genes involved in lipid homeostasis, energy metabolism, inflammatory response, apoptosis, and its expression was observed in normal adrenals, benign adrenocortical tumors, ACC [47] and in the NCI-H295R cell line [8]. *PPARG* coactivator 1A (*PPARGC1A*) gene, a transcription coactivator of the nuclear receptor *PPARG* was upregulated by 9-*cis*RA treatment and downregulated in one microarray study [21].

Cell cycle

Cell-cycle damage has been described in many tumors including ACC [21]. We have found significant changes associated with cell-cycle regulation following 9-*cis*RA treatment in ataxia telangiectasia mutated (*ATM*) signaling, growth arrest and DNA-damage-inducible (*GADD45*)

Table 1 Summary of the most important pathways and gene expression results along with inverse expression alterations in reported functional genomics data in ACA-ACC comparison

Gene symbol	Gene name	Expression changes after 9- <i>cis</i> RA treatment of NCI-H295R cells in our study	Inverse expression changes in previously published microarray studies in the ACA-ACC comparison [References]
(1) Steroid hormone metabolism			
<i>CYP11A1</i>	<i>Cytochrome P450 side chain cleavage enzyme (scc)</i>	↓	
<i>CYP11B2</i>	<i>Steroid 11-beta-monooxygenase</i>	↓	
<i>CYP17A1</i>	<i>Steroid 17-alpha-monooxygenase</i>	↓	
<i>EBP</i>	<i>Emopamil binding protein</i>	↓	
<i>HSD11B2</i>	<i>Hydroxysteroid (11-beta) dehydrogenase 2</i>	↓	
<i>HSD3B1</i>	<i>Hydroxy-delta-5-steroid dehydrogenase, 3 beta- and steroid delta-isomerase 1</i>	↓	
<i>HSD3B2</i>	<i>Hydroxy-delta-5-steroid dehydrogenase, 3 beta- and steroid delta-isomerase 2</i>	↓	↑ [40]
<i>HSD11B2</i>	<i>Hydroxysteroid (11-beta) dehydrogenase 2</i>	↓	
(2) Retinoic acid signaling			
<i>ABCA1</i>	<i>ATP-binding cassette, sub-family A, member 1</i>	↑	↓ [19–21, 27]
<i>ABCC3</i>	<i>ATP-binding cassette, sub-family C (CFTR/MRP), member 3</i>	↑	↓ [19–22, 25–27]
<i>ABCG1</i>	<i>ATP-binding cassette, sub-family G, member 1</i>	↑	↓ [19–21]
<i>ALDH1A1</i>	<i>Aldehyde dehydrogenase 1 family, member A1</i>	↑	↓ [18, 19, 22, 24–26]
<i>HMGR</i>	<i>3-hydroxy-3-methylglutaryl-CoA reductase</i>	↓	
<i>LXRA</i>	<i>Liver X receptor alpha</i>	↓	
<i>LXRB</i>	<i>Liver X receptor beta</i>	↑	
<i>PPARG</i>	<i>Peroxisome proliferator-activated receptor gamma</i>	↑	
<i>PPARGC1A</i>	<i>Peroxisome proliferator-activated receptor gamma, coactivator 1 alpha</i>	↑	↓ [20]
(3) Cell cycle			
<i>CCNB2</i>	<i>Cyclin B2</i>	↓	↑ [18–21, 26]
<i>CCNE1</i>	<i>Cyclin E1</i>	↓	↑ [18–21]
<i>CCNE2</i>	<i>Cyclin E2</i>	↓	↑ [19, 20]
<i>CDK1</i>	<i>Cyclin-dependent kinase 1</i>	↓	↑ [18–21, 26]
<i>c-FOS</i>	<i>Cellular oncogene Fos</i>	↑	↓ [18, 19]
<i>c-MYC</i>	<i>Cellular myelocytomatosis oncogene</i>	↑	↓ [18–20, 24]
<i>E2F2</i>	<i>E2F transcription factor 2</i>	↓	↑ [20]
<i>GADD45A</i>	<i>Growth arrest and DNA-damage-inducible, alpha</i>	↑	
<i>SKP2</i>	<i>S-phase kinase-associated protein 2</i>	↓	↑ [19, 20]
<i>TP53</i>	<i>Tumor protein p53</i>	↑	
<i>UHRF1</i>	<i>Ubiquitin-like with PHD and ring finger domains 1</i>	↓	↑ [18–20, 26]
(4) Immune response			
<i>CD14</i>	<i>CD14</i>	↑	↓ [18–21, 58]
<i>IL-1R2</i>	<i>Interleukin 1 receptor, type II</i>	↓	↑ [20]
<i>LY96</i>	<i>Lymphocyte antigen 96</i>	↑	↓ [18]
<i>MAP2K6</i>	<i>Mitogen-activated protein kinase kinase 6</i>	↓	
<i>TLR4</i>	<i>Toll-like receptor 4</i>	↑	↓ [19, 20, 58]

Real-time PCR validated genes are highlighted in bold

signaling, aryl hydrocarbon receptor (AHR) signaling, cyclins and cell-cycle regulation and the estrogen-mediated S-phase entry pathways.

AHR-mediated changes of gene expression affect cell growth and cell-cycle control [48]. ATM signaling is one of the most important pathways in the induction of cellular

DNA damage responses. ATM plays a crucial role in cell-cycle regulation, DNA repair, transcription, and apoptosis via the ATM-mediated phosphorylation of a number of proteins, including GADD45 and tumor suppressors like TP53 [49]. GADD45 proteins (GADD45A, GADD45B, and GADD45G) are stress sensors that participate in cell-cycle arrest, DNA repair, cell survival, and apoptosis [50]. We have validated the 9-*cis*RA-induced overexpression of the *GADD45A* gene by qRT-PCR. *TP53* is one of the most well-known tumor suppressor genes that is involved in the control of cell proliferation and implicated in the pathogenesis of many tumors including ACC [3]. We have observed *TP53* gene overexpression after 9-*cis*RA treatment.

Another major pathway is related to damage of cell-cycle checkpoint regulations. There are reports of expression changes of genes involved in the G1/S and G2/M transitions in ACC [7, 21]. S-phase kinase-associated protein 2 (SKP2) and UHRF1 are involved in the regulation of G1/S checkpoint. SKP2 is a bona fide proto-oncoprotein that is a component of the SCF E3 ubiquitin ligase complex and its overexpression has been observed in different forms of human cancer [51]. We have found down-regulation of *SKP2* gene after 9-*cis*RA treatment, whereas it has been overexpressed in ACC in two microarray studies [20, 21]. *UHRF1* is down-regulated by the TP53, and is overexpressed in many types of cancer. Knockdown of *UHRF1* expression in cancer cells suppressed cell growth, suggesting that *UHRF1* can be a potential anticancer drug target [52]. We have found the overexpression of *UHRF1* in ACC in four microarray studies [19–21, 27] compared to its 9-*cis*RA-induced underexpression in vitro that has been successfully validated by qRT-PCR. After 9-*cis*RA treatment, expression of several members of the G2/M checkpoint regulatory system has been altered in several microarray studies in ACC: *CDK1* [19–22, 27], *CCNE1* [19–22], *CCNE2* [20, 21], and *CCNB2* [19–22, 27]. All of them were underexpressed after 9-*cis*RA treatment and overexpressed in the microarray studies in ACC. We have validated the underexpression of the *CCNE2* gene.

We have also found that the expression of transcription factor genes like *c-MYC*, *c-FOS*, and *E2F transcription factor 2 (E2F2)* was altered by 9-*cis*RA treatment. In our previous meta-analysis on ACC genomics data, underexpression of *c-MYC* has been observed, and by network analysis it has been identified as a major hub in gene expression networks [7, 53]. We found significant overexpression of the *c-MYC* gene after 9-*cis*RA treatment compared to its significant underexpression in ACC in four microarray studies [19–21, 25]. We also found significant up-regulation of *c-FOS* after 9-*cis*RA treatment and its down-regulation in two microarray studies in ACC [19, 20]. Earlier mice and human studies suggest that E2F2 function as a tumor suppressor and can be transcriptionally activated by the

c-MYC oncoprotein [54]. The *E2F2* gene was significantly down-regulated after 9-*cis*RA treatment and significantly overexpressed in one microarray study in ACC [21].

Based on our network analysis, the changes in the cell cycle are directly elicited by the 9-*cis*RA treatment and not via its effects on hormone secretion. In the network hierarchy top region, we identified two 9-*cis*RA receptor transcription factor complexes (LXR-RXRA and NCOR-LXR-RXR) as master regulators the core and bottom levels, and mostly genes involved in cell-cycle regulation are found that are all under 9-*cis*RA regulation. Moreover, three motifs cross the network hierarchy top-core-bottom layers, which are feed-forward loop motifs. The feed-forward loop is one of the most significant network motifs that is commonly found in many gene systems and organisms [55].

Immune response

Following 9-*cis*RA treatment, changes of the immune response in the p38 mitogen-activated protein family of kinases (p38 MAPK) signaling and in the macrophage migration inhibitory factor (MIF) regulation of innate immunity pathways have been identified.

p38 MAPK signaling plays important roles in immune response as well as in the regulation of cell proliferation, differentiation, and cell survival. MAP2K6 plays a major role in p38 MAPK activation [56]. We have found a significant, concentration-dependent decrease in *MAP2K6* gene expression by 9-*cis*RA treatment, and we have successfully validated this by qRT-PCR.

MIF is a T-cell cytokine that is an important modulator of innate and adaptive immune responses. MIF decreases the production of several cytokines by down-regulating the expression of Toll-like receptor 4 (TLR4) [57]. Lipopolysaccharide (LPS) is a known activator of TLR4. CD14 and LY96 are required [58] for the TLR4-mediated immune response. *TLR4* [20, 21], *CD14* [19–22], and *LY96* [19] genes were found to be underexpressed in several microarray studies in ACC, but all three have been overexpressed after 9-*cis*RA treatment. Underexpression of *TLR4* and *CD14* genes were reported in ACC [59].

The IL-1 cytokine is a major proinflammatory cytokine that is involved in the immune-neuroendocrine crosstalk [60]. IL-1 can bind to IL-1 type 1 and IL-1 type 2 receptors (IL-1R1 and IL-1R2), but IL-1R2 is a functionally inactive, decoy receptor [61]. We have found significant overexpression of *IL-1R2* in ACC in one microarray study [21], whereas 9-*cis*RA treatment resulted in its significant underexpression in NCI-H295R cells that could be validated by qRT-PCR.

In our present experiments with 9-*cis*RA and in our previous in vitro study on mitotane [17], both agents were

effective in inhibiting hormone secretion and decreasing cell viability. In our study on the genomic actions of mitotane in NCI-H295R cells, mitotane affected the expression of much fewer genes than 9-*cis*RA did. The mechanism of action of mitotane is poorly understood despite being used for more than 50 years in clinical practice [6]. Whereas 9-*cis*RA seems to have multifaceted effects on gene expression, the genomic effects of mitotane appear to be modest, mainly affecting the expression of steroid biosynthetic enzymes. The more profound genomic effects of 9-*cis*RA certainly do not indicate its superiority over mitotane, as mitotane affects numerous other basic cell biological processes. We do not think that the results of in vitro experiments can be extrapolated to the in vivo setting, and therefore we cannot conclude that 9-*cis*RA might be a better treatment option for ACC than mitotane based on in vitro studies.

Clinical observations, however, clearly show that 9-*cis*RA is well tolerated and effective with much less severe side effects than mitotane. The most frequent side effects of 9-*cis*RA include headache and mucocutaneous adverse events (dry lips, cheilitis, and dry skin) [62], whereas mitotane is associated mainly with gastrointestinal (nausea, vomiting, diarrhea, anorexia, mucositis, etc.) or central nervous system (lethargy, somnolence, vertigo, ataxia etc.) complications that can be severe [6]. The therapeutic window of mitotane is narrow (14–20 mg/l serum concentration) [6]. Serum concentration monitoring is not required for current treatment protocols using 9-*cis*RA. The applicability of 9-*cis*RA in ACC treatment should be examined in further animal studies and clinical trials.

Conclusions

Based on these observations, 9-*cis*RA might be a promising novel candidate for the treatment of ACC as it inhibited both cell proliferation and hormone secretion in vitro, and several pathways appear to be regulated in 9-*cis*RA action. The in vivo pilot xenograft study seems to corroborate the antitumoral activity of 9-*cis*RA, but further studies are needed to investigate the applicability of 9-*cis*RA in the treatment of adrenocortical cancer.

Acknowledgments This study has been funded by the Hungarian Scientific Research Fund (OTKA K100295).

References

- Fassnacht M, Libe R, Kroiss M, Allolio B (2011) Adrenocortical carcinoma: a clinician's update. *Nat Rev Endocrinol* 7(6):323–335. doi:10.1038/nrendo.2010.235
- Lafemina J, Brennan MF (2012) Adrenocortical carcinoma: past, present, and future. *J Surg Oncol* 106(5):586–594. doi:10.1002/jso.23112
- Libe R, Fratticci A, Bertherat J (2007) Adrenocortical cancer: pathophysiology and clinical management. *Endocr Relat Cancer* 14(1):13–28. doi:10.1677/erc.1.01130
- Fassnacht M, Terzolo M, Allolio B, Baudin E, Haak H, Berruti A, Welin S, Schade-Brittinger C, Lacroix A, Jarzab B, Sorbye H, Torpy DJ, Stepan V, Schteingart DE, Arlt W, Kroiss M, Lebloulloux S, Sperone P, Sundin A, Hermsen I, Hahner S, Willenberg HS, Tabarin A, Quinkler M, de la Fouchardiere C, Schlumberger M, Mantero F, Weismann D, Beuschlein F, Gelderblom H, Wilmink H, Sender M, Edgerly M, Kenn W, Fojo T, Muller HH, Skogseid B (2012) Combination chemotherapy in advanced adrenocortical carcinoma. *N Engl J Med* 366(23):2189–2197. doi:10.1056/NEJMoa1200966
- Terzolo M, Ardito A, Zaggia B, Laino F, Germano A, De Francia S, Daffara F, Berruti A (2012) Management of adjuvant mitotane therapy following resection of adrenal cancer. *Endocrine* 42(3):521–525. doi:10.1007/s12020-012-9719-7
- Hahner S, Fassnacht M (2005) Mitotane for adrenocortical carcinoma treatment. *Curr Opin Investig Drugs* 6(4):386–394
- Szabo PM, Tamasi V, Molnar V, Andrasfalvy M, Tombol Z, Farkas R, Kovessi K, Patocs A, Toth M, Szalai C, Falus A, Racz K, Igaz P (2010) Meta-analysis of adrenocortical tumour genomics data: novel pathogenic pathways revealed. *Oncogene* 29(21):3163–3172. doi:10.1038/onc.2010.80
- Ferruzzi P, Ceni E, Tarocchi M, Grappone C, Milani S, Galli A, Fiorelli G, Serio M, Mannelli M (2005) Thiazolidinediones inhibit growth and invasiveness of the human adrenocortical cancer cell line H295R. *J Clin Endocrinol Metab* 90(3):1332–1339. doi:10.1210/jc.2004-0978
- Perez E, Bourguet W, Gronemeyer H, de Lera AR (2012) Modulation of RXR function through ligand design. *Biochim Biophys Acta* 1821(1):57–69. doi:10.1016/j.bbali.2011.04.003
- Shimizu M, Takai K, Moriwaki H (2009) Strategy and mechanism for the prevention of hepatocellular carcinoma: phosphorylated retinoid X receptor alpha is a critical target for hepatocellular carcinoma chemoprevention. *Cancer Sci* 100(3):369–374. doi:10.1111/j.1349-7006.2008.01045.x
- Ganslmayer M, Ocker M, Kraemer G, Zopf S, Hahn EG, Schuppan D, Herold C (2004) The combination of tamoxifen and 9-*cis* retinoic acid exerts overadditive anti-tumoral efficacy in rat hepatocellular carcinoma. *J Hepatol* 40(6):952–956. doi:10.1016/j.jhep.2004.02.004
- Tatebe H, Shimizu M, Shirakami Y, Tsurumi H, Moriwaki H (2008) Synergistic growth inhibition by 9-*cis*-retinoic acid plus trastuzumab in human hepatocellular carcinoma cells. *Clin Cancer Res* 14(9):2806–2812. doi:10.1158/1078-0432.CCR-07-4708
- Cope MB, Steele VE, Lubet RA, Eto I, Juliana MM, Hill DL, Grubbs CJ (2004) Efficacy of 9-*cis*-retinoic acid and *N*-(4-hydroxyphenyl) retinamide alone and in combination in mammary cancer prevention. *Oncol Rep* 11(2):465–469
- Maeng S, Kim GJ, Choi EJ, Yang HO, Lee DS, Sohn YC (2012) 9-*Cis*-retinoic acid induces growth inhibition in retinoid-sensitive breast cancer and sea urchin embryonic cells via retinoid X receptor alpha and replication factor C3. *Mol Endocrinol* 26(11):1821–1835. doi:10.1210/me.2012-1104
- Fatahzadeh M (2011) Kaposi sarcoma: review and medical management update. *Oral Surg Oral Med Oral Pathol Oral Radiol Endod.* doi:10.1016/j.tripleo.2011.05.011
- Lawrence JA, Adamson PC, Caruso R, Chow C, Kleiner D, Murphy RF, Venzon DJ, Shovlin M, Noone M, Merino M, Cowan KH, Kaiser M, O'Shaughnessy J, Zujewski J (2001) Phase

- I clinical trial of alitretinoin and tamoxifen in breast cancer patients: toxicity, pharmacokinetic, and biomarker evaluations. *J Clin Oncol* 19(10):2754–2763
17. Zsippai A, Szabo DR, Tombol Z, Szabo PM, Eder K, Pallinger E, Gaillard RC, Patocs A, Toth S, Falus A, Racz K, Igaz P (2012) Effects of mitotane on gene expression in the adrenocortical cell line NCI-H295R: a microarray study. *Pharmacogenomics* 13(12):1351–1361. doi:10.2217/pgs.12.116
 18. Goon PK, Boos CJ, Stonelake PS, Blann AD, Lip GY (2006) Detection and quantification of mature circulating endothelial cells using flow cytometry and immunomagnetic beads: a methodological comparison. *Thromb Haemost* 96(1):45–52. doi:10.1160/TH06-04-0185
 19. de Reynies A, Assie G, Rickman DS, Tissier F, Groussin L, Rene-Corail F, Dousset B, Bertagna X, Clauser E, Bertherat J (2009) Gene expression profiling reveals a new classification of adrenocortical tumors and identifies molecular predictors of malignancy and survival. *J Clin Oncol* 27(7):1108–1115. doi:10.1200/JCO.2008.18.5678
 20. Giordano TJ, Kuick R, Else T, Gauger PG, Vinco M, Bauersfeld J, Sanders D, Thomas DG, Doherty G, Hammer G (2009) Molecular classification and prognostication of adrenocortical tumors by transcriptome profiling. *Clin Cancer Res* 15(2):668–676. doi:10.1158/1078-0432.CCR-08-1067
 21. Tombol Z, Szabo PM, Molnar V, Wiener Z, Tolgyesi G, Horanyi J, Riesz P, Reismann P, Patocs A, Liko I, Gaillard RC, Falus A, Racz K, Igaz P (2009) Integrative molecular bioinformatics study of human adrenocortical tumors: microRNA, tissue-specific target prediction, and pathway analysis. *Endocr Relat Cancer* 16(3):895–906. doi:10.1677/ERC-09-0096
 22. Giordano TJ, Thomas DG, Kuick R, Lizyness M, Misek DE, Smith AL, Sanders D, Aljundi RT, Gauger PG, Thompson NW, Taylor JM, Hanash SM (2003) Distinct transcriptional profiles of adrenocortical tumors uncovered by DNA microarray analysis. *Am J Pathol* 162(2):521–531. doi:10.1016/S0002-9440(10)63846-1
 23. Fernandez-Ranvier GG, Weng J, Yeh RF, Khanafshar E, Suh I, Barker C, Duh QY, Clark OH, Kebebew E (2008) Identification of biomarkers of adrenocortical carcinoma using genomewide gene expression profiling. *Arch Surg* 143(9):841–846. doi:10.1001/archsurg.143.9.841 (discussion 846)
 24. Fernandez-Ranvier GG, Weng J, Yeh RF, Shibru D, Khanafshar E, Chung KW, Hwang J, Duh QY, Clark OH, Kebebew E (2008) Candidate diagnostic markers and tumor suppressor genes for adrenocortical carcinoma by expression profile of genes on chromosome 11q13. *World J Surg* 32(5):873–881. doi:10.1007/s00268-008-9521-0
 25. Laurell C, Velazquez-Fernandez D, Lindsten K, Juhlin C, Enberg U, Geli J, Hoog A, Kjellman M, Lundberg J, Hamberger B, Larsson C, Nilsson P, Backdahl M (2009) Transcriptional profiling enables molecular classification of adrenocortical tumours. *Eur J Endocrinol* 161(1):141–152. doi:10.1530/EJE-09-0068
 26. Slater EP, Diehl SM, Langer P, Samans B, Ramaswamy A, Zielke A, Bartsch DK (2006) Analysis by cDNA microarrays of gene expression patterns of human adrenocortical tumors. *Eur J Endocrinol* 154(4):587–598. doi:10.1530/eje.1.02116
 27. Soon PS, Gill AJ, Benn DE, Clarkson A, Robinson BG, McDonald KL, Sidhu SB (2009) Microarray gene expression and immunohistochemistry analyses of adrenocortical tumors identify IGF2 and Ki-67 as useful in differentiating carcinomas from adenomas. *Endocr Relat Cancer* 16(2):573–583. doi:10.1677/ERC-08-0237
 28. West AN, Neale GA, Pounds S, Figueredo BC, Rodriguez Galindo C, Pianovski MA, Oliveira Filho AG, Malkin D, Lalli E, Ribeiro R, Zambetti GP (2007) Gene expression profiling of childhood adrenocortical tumors. *Cancer Res* 67(2):600–608. doi:10.1158/0008-5472.CAN-06-3767
 29. Friedel CC, Zimmer R (2007) Influence of degree correlations on network structure and stability in protein–protein interaction networks. *BMC Bioinforma* 8:297. doi:10.1186/1471-2105-8-297
 30. Jothi R, Balaji S, Wuster A, Grochow JA, Gsponer J, Przytycka TM, Aravind L, Babu MM (2009) Genomic analysis reveals a tight link between transcription factor dynamics and regulatory network architecture. *Mol Syst Biol* 5:294. doi:10.1038/msb.2009.52
 31. Milo R, Shen-Orr S, Itzkovitz S, Kashtan N, Chklovskii D, Alon U (2002) Network motifs: simple building blocks of complex networks. *Science* 298(5594):824–827. doi:10.1126/science.298.5594.824
 32. Ayaori M, Yakushiji E, Ogura M, Nakaya K, Hisada T, Uto-Kondo H, Takiguchi S, Terao Y, Sasaki M, Komatsu T, Iizuka M, Yogo M, Uehara Y, Kagechika H, Nakanishi T, Ikekawa K (2012) Retinoic acid receptor agonists regulate expression of ATP-binding cassette transporter G1 in macrophages. *Biochim Biophys Acta* 1821(4):561–572. doi:10.1016/j.bbali.2012.02.004
 33. Livak KJ, Schmittgen TD (2001) Analysis of relative gene expression data using real-time quantitative PCR and the 2(-Delta Delta C(T)) method. *Methods* 25(4):402–408. doi:10.1006/meth.2001.1262
 34. Larionov A, Krause A, Miller W (2005) A standard curve-based method for relative real-time PCR data processing. *BMC Bioinforma* 6:62. doi:10.1186/1471-2105-6-62
 35. Cheng WC, Chang CW, Chen CR, Tsai ML, Shu WY, Li CY, Hsu IC (2011) Identification of reference genes across physiological states for qRT-PCR through microarray meta-analysis. *PLoS ONE* 6(2):e17347. doi:10.1371/journal.pone.0017347
 36. Logie A, Boudou P, Boccon-Gibod L, Baudin E, Vassal G, Schlumberger M, Le Bouc Y, Gicquel C (2000) Establishment and characterization of a human adrenocortical carcinoma xenograft model. *Endocrinology* 141(9):3165–3171
 37. Luconi M, Mangoni M, Gelmini S, Poli G, Nesi G, Francalanci M, Pratesi N, Cantini G, Lombardi A, Pepi M, Ercolino T, Serio M, Orlando C, Mannelli M (2010) Rosiglitazone impairs proliferation of human adrenocortical cancer: preclinical study in a xenograft mouse model. *Endocr Relat Cancer* 17(1):169–177. doi:10.1677/ERC-09-0170
 38. Appleyard VC, O'Neill MA, Murray KE, Bray SE, Thomson G, Kernohan NM, Varani J, Zhang J, Thompson AM (2004) Activity of MDI-301, a novel synthetic retinoid, in xenografts. *Anticancer Drugs* 15(10):991–996 (pii:00001813-200411000-00009)
 39. Gazdar AF, Oie HK, Shackleton CH, Chen TR, Triche TJ, Myers CE, Chrousos GP, Brennan MF, Stein CA, La Rocca RV (1990) Establishment and characterization of a human adrenocortical carcinoma cell line that expresses multiple pathways of steroid biosynthesis. *Cancer Res* 50(17):5488–5496
 40. Simard JRM, Gingras S, Soucy P, Feltus FA, Melner MH (2005) Molecular biology of the 3 β -hydroxysteroid dehydrogenase/ Δ 5- Δ 4 isomerase gene family. *Endocr Rev* 26(4):525–582
 41. Bassett MH, Mayhew B, Rehman K, White PC, Mantero F, Arnaldi G, Stewart PM, Bujalska I, Rainey WE (2005) Expression profiles for steroidogenic enzymes in adrenocortical disease. *J Clin Endocrinol Metab* 90(9):5446–5455. doi:10.1210/jc.2005-0836
 42. Lefevre A, Rogier E, Astraudo C, Duquenne C, Finaz C (1994) Regulation by retinoids of luteinizing hormone/chorionic gonadotropin receptor, cholesterol side-chain cleavage cytochrome P-450, 3 beta-hydroxysteroid dehydrogenase/delta (5-4)-isomerase and 17 alpha-hydroxylase/C17-20 lyase cytochrome P-450 messenger ribonucleic acid levels in the K9 mouse Leydig cell line. *Mol Cell Endocrinol* 106(1–2):31–39
 43. Paez-Pereda M, Kovalovsky D, Hopfner U, Theodoropoulou M, Pagotto U, Uhl E, Losa M, Stalla J, Grubler Y, Missale C, Arzt

- E, Stalla GK (2001) Retinoic acid prevents experimental Cushing syndrome. *J Clin Invest* 108(8):1123–1131. doi:[10.1172/jci11098](https://doi.org/10.1172/jci11098)
44. Cummins CL, Volle DH, Zhang Y, McDonald JG, Sion B, Lefrançois-Martinez AM, Caira F, Veyssiere G, Mangelsdorf DJ, Lobb JC, Lobb JC (2006) Liver X receptors regulate adrenal cholesterol balance. *J Clin Invest* 116(7):1902–1912. doi:[10.1172/JCI28400](https://doi.org/10.1172/JCI28400)
 45. Tojima H, Kakizaki S, Yamazaki Y, Takizawa D, Horiguchi N, Sato K, Mori M (2012) Ligand-dependent hepatic gene expression profiles of nuclear receptors CAR and PXR. *Toxicol Lett* 212(3):288–297. doi:[10.1016/j.toxlet.2012.06.001](https://doi.org/10.1016/j.toxlet.2012.06.001)
 46. Aleksunes LM, Klaassen CD (2012) Coordinated regulation of hepatic phase I and II drug-metabolizing genes and transporters using AhR-, CAR-, PXR-, PPARalpha-, and Nrf2-null mice. *Drug Metab Dispos* 40(7):1366–1379. doi:[10.1124/dmd.112.045112](https://doi.org/10.1124/dmd.112.045112)
 47. Yamazaki K, Shimizu M, Okuno M, Matsushima-Nishiwaki R, Kanemura N, Araki H, Tsurumi H, Kojima S, Weinstein IB, Moriwaki H (2007) Synergistic effects of RXR alpha and PPAR gamma ligands to inhibit growth in human colon cancer cells—phosphorylated RXR alpha is a critical target for colon cancer management. *Gut* 56(11):1557–1563. doi:[10.1136/gut.2007.129858](https://doi.org/10.1136/gut.2007.129858)
 48. Elferink CJ (2003) Aryl hydrocarbon receptor-mediated cell cycle control. *Prog Cell Cycle Res* 5:261–267
 49. Jang ER, Choi JD, Park MA, Jeong G, Cho H, Lee JS (2010) ATM modulates transcription in response to histone deacetylase inhibition as part of its DNA damage response. *Exp Mol Med* 42(3):195–204 pii:emm.2010.42.020
 50. Liebermann DA, Tront JS, Sha X, Mukherjee K, Mohamed-Hadley A, Hoffman B (2011) Gadd45 stress sensors in malignancy and leukemia. *Crit Rev Oncog* 16(1–2):129–140 (pii:049e8a5e62fb019e,70f927fe5a67ad86)
 51. Wang G, Chan CH, Gao Y, Lin HK (2012) Novel roles of Skp2 E3 ligase in cellular senescence, cancer progression, and metastasis. *Chin J Cancer* 31(4):169–177. doi:[10.5732/cjc.011.10319](https://doi.org/10.5732/cjc.011.10319)
 52. Unoki M, Brunet J, Mousli M (2009) Drug discovery targeting epigenetic codes: the great potential of UHRF1, which links DNA methylation and histone modifications, as a drug target in cancers and toxoplasmosis. *Biochem Pharmacol* 78(10):1279–1288. doi:[10.1016/j.bcp.2009.05.035](https://doi.org/10.1016/j.bcp.2009.05.035)
 53. Szabo PM, Racz K, Igaz P (2011) Underexpression of C-myc in adrenocortical cancer: a major pathogenic event? *Horm Metab Res* 43(5):297–299. doi:[10.1055/s-0031-1273762](https://doi.org/10.1055/s-0031-1273762)
 54. Pusapati RV, Weaks RL, Rounbehler RJ, McArthur MJ, Johnson DG (2010) E2F2 suppresses Myc-induced proliferation and tumorigenesis. *Mol Carcinog* 49(2):152–156. doi:[10.1002/mc.20584](https://doi.org/10.1002/mc.20584)
 55. Mangan S, Alon U (2003) Structure and function of the feed-forward loop network motif. *Proc Natl Acad Sci USA* 100(21):11980–11985. doi:[10.1073/pnas.2133841100](https://doi.org/10.1073/pnas.2133841100)
 56. Cuadrado A, Nebreda AR (2010) Mechanisms and functions of p38 MAPK signalling. *Biochem J* 429(3):403–417. doi:[10.1042/BJ20100323](https://doi.org/10.1042/BJ20100323)
 57. Popa C, van Lieshout AW, Roelofs MF, Geurts-Moespot A, van Riel PL, Calandra T, Sweep FC, Radstake TR (2006) MIF production by dendritic cells is differentially regulated by Toll-like receptors and increased during rheumatoid arthritis. *Cytokine* 36(1–2):51–56. doi:[10.1016/j.cyto.2006.10.011](https://doi.org/10.1016/j.cyto.2006.10.011)
 58. Hankins JL, Fox TE, Barth BM, Unrath KA, Kester M (2011) Exogenous ceramide-1-phosphate reduces lipopolysaccharide (LPS)-mediated cytokine expression. *J Biol Chem* 286(52):44357–44366. doi:[10.1074/jbc.M111.264010](https://doi.org/10.1074/jbc.M111.264010)
 59. Kanczkowski W, Tymoszek P, Ehrhart-Bornstein M, Wirth MP, Zacharowski K, Bornstein SR (2010) Abrogation of TLR4 and CD14 expression and signaling in human adrenocortical tumors. *J Clin Endocrinol Metab* 95(12):E421–E429. doi:[10.1210/jc.2010-1100](https://doi.org/10.1210/jc.2010-1100)
 60. John CD, Buckingham JC (2003) Cytokines: regulation of the hypothalamo-pituitary-adrenocortical axis. *Curr Opin Pharmacol* 3(1):78–84 (pii:S1471489202000097)
 61. O’Neill LA (2008) The interleukin-1 receptor/Toll-like receptor superfamily: 10 years of progress. *Immunol Rev* 226:10–18. doi:[10.1111/j.1600-065X.2008.00701.x](https://doi.org/10.1111/j.1600-065X.2008.00701.x)
 62. Bissonnette R, Worm M, Gerlach B, Guenther L, Cambazard F, Ruzicka T, Maares J, Brown TC (2010) Successful retreatment with alitretinoin in patients with relapsed chronic hand eczema. *Br J Dermatol* 162(2):420–426. doi:[10.1111/j.1365-2133.2009.09572.x](https://doi.org/10.1111/j.1365-2133.2009.09572.x)